Acta Mechanica Solida Sinica, Vol. 23, No. 2, April, 2010 ISSN 0894-9166
Published by AMSS Press, Wuhan, China.

LOCAL BENDING OF THIN FILM ON VISCOUS LAYER**

Yin Zhang[1]* **Yun Liu**[2]

([1] *State Key Laboratory of Nonlinear Mechanics (LNM), Institute of Mechanics, Chinese Academy of Sciences, Beijing* 100190*, China*)

([2] *Faculty of Information and Automation, Kunming University of Science and Technology, Kunming* 650051*, China*)

Received 2 March 2009, revision received 4 December 2009

ABSTRACT Effects of deposition layer position and number/density on local bending of a thin film are systematically investigated. Because the deposition layer interacts with the thin film at the interface and there is an offset between the thin film neutral surface and the interface, the deposition layer generates not only axial stress but also bending moment. The bending moment induces an instant out-of-plane deflection of the thin film, which may or may not cause the so-called local bending. The deposition layer is modeled as a local stressor, whose location and density are demonstrated to be vital to the occurrence of local bending. The thin film rests on a viscous layer, which is governed by the Navier-Stokes equation and behaves like an elastic foundation to exert transverse forces on the thin film. The unknown feature of the axial constraint force makes the governing equation highly nonlinear even for the small deflection case. The constraint force and film transverse deflection are solved iteratively through the governing equation and the displacement constraint equation of immovable edges. This research shows that in some special cases, the deposition density increase does not necessarily reduce the local bending. By comparing the thin film deflections of different deposition numbers and positions, we also present the guideline of strengthening or suppressing the local bending.

KEY WORDS local bending, deposition layer/dot, thin film, viscous layer, constraint

I. INTRODUCTION

The lattice mismatch of different materials has been used as a driving mechanism to grow quantum dots, or say, nanoscale clusters[1–6]. The stress/strain at the bimaterial interface induced by the lattice mismatch can also cause wrinkling, or variably called corrugation, undulation, convolution and ripples of a thin film[7–11]. Liu et al.[11] reported that germanium (Ge) deposition dots on the compliant thin silicon film of Silicon-on-Insulator (SOI) substrates cause the local bending mode of a compliant film as shown in Fig.1. The SOI substrate in Ref.[11] consists of a thin silicon (Si) layer, a thin silicon oxide layer and a thick silicon handle wafer layer. The silicon oxide layer at 700 °C (its growth temperature) is modeled as a viscous fluid[6, 11]. The effect of a Ge dot on a thin compliant film is modeled as a local stressor[11]. The 4.2% lattice mismatch[11] and intermixing/alloying effects of Ge and Si[5, 6] result in the stress/strain at the bimaterial interface, which offers a driving mechanism for the film morphology

* Corresponding author. E-mail: zhangyin@lnm.imech.ac.cn

** Project supported by the National Natural Science Foundation of China (No.10721202) and the LNM Initial Funding for Young Investigators.

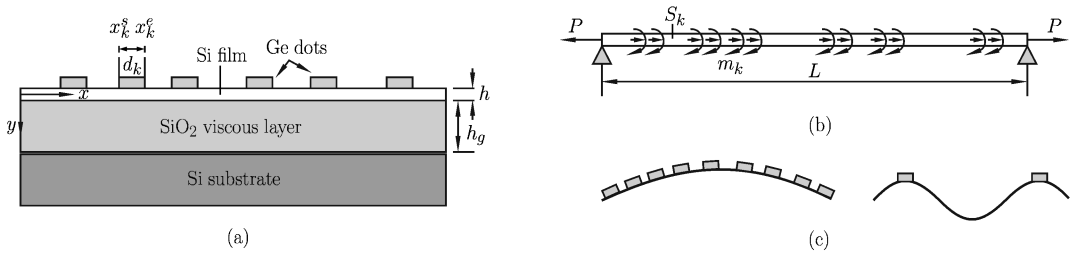

Fig. 1. (a) Schematic illustration of Ge depositions on a Si thin film. The thin film is on a SiO2 viscous layer, which rests on a solid and rigid Si substrate. The thin film dimensions and coordinates, Ge deposition layer dimensions are also shown. (b) The distributed stress and bending moment exerted by the Ge deposition layers on the thin film. (c) The scenarios of the overall and local bendings. In the overall bending the curvature does not change its sign and there are sign changes in the curvature of the local bending.

evolution[12,13]. Because the local bending results in an undulating strain field inside a thin film, the formation of a potential well can influence the development of quantum dots[14]. Also, the strain can alter the crystal symmetry and shift the electronic band, the electronic properties of the thin film can be significantly changed[14,15], especially when the local bending is formed. The offset between the interface and the film neutral surface induces a bending moment in the Ge deposition area, which causes an instant bending of the thin film layer. The previous models on the film morphology[12,13,16] are the stability analysis, which are the non-equilibrium analysis and offer no information on the nature of the steady-state film profile[13]. Because there is stress concentration around the valleys of a (sinusoidal) thin film, Yang and Srolovitz[17] presented a model which goes beyond the stability analysis and is capable of describing the film cusp-forming morphology evolution via a fracture mechanics approach. The models presented by Huang and Suo treat the viscous layer either by the lubrication theory[18] or as the Stokes flow[19]. In Huang and Suo's models as discussed later, the viscous layer is equivalent to an elastic foundation offering a transverse support to the upper thin film layer and their two models are also capable of describing the temporal evolution of film morphology. The elastic foundation model is also used by Huck et al.[20] in the wrinkling forming study of a metal film on a polydimethylsiloxane (PDMS) substrate. In Huang and Suo's models[18,19], the film governing equation is a static one and the morphology evolution is implicitly embodied in the viscous layer. This study offers an equilibrium/static study which addresses the influences of the location and density of the deposition layers on the deflection of the thin film. Therefore, the viscous layer here is assumed in a steady state. In those models[18–20], wrinkling is formed because of the buckling/postbuckling of the thin film when compressive axial stress surpasses the critical value. Our model incorporates the bending moments induced by the deposition layers, which cause the out-of-plane deflection instantly no matter what the axial stress state is. As shown later in the paper, once the bending moment is removed, our analysis recovers the buckling analysis by Huang and Suo[18,19]. The constraint has been demonstrated to have huge influence on the wrinkling pattern of the thin film on compliant substrates[20,21]. In this paper the immovable edge constraint is imposed, which also implicitly indicates that the film edges are not delaminated. The boundary conditions and the film length also play important roles of the film/substrate bilayer deflection induced by the interfacial stress[22], which are also incorporated in this model. It is noticed that in Huang and Suo's perturbation solutions[18,19] periodic boundary conditions are implicitly assumed.

Liu et al.[11] also reported that the local bending (curvature) depends on the Ge deposition layer/dot density and shapes. In this paper a systematic study on the effects of Ge deposition layers/dots and the viscous SiO_2 layer on the wrinkling of a thin film is presented. Our model and computation results in general agree with the experimental report by Liu et al.[11] that local bending tends to evolve to an overall extended bending as the Ge layer/dot density increases. However, our model also shows that in some special cases increasing Ge dots density may not necessarily reduce local bending. We analyze and compare the deposition position influence on both the symmetric and anti-symmetric mode shapes of a thin film. We show that in many cases the deposition layer/dot positions play a very important role in the local bending of a thin film, which can be used as a guide to strengthen or weaken/suppress the local bending.

II. MODEL DEVELOPMENT

2.1. Equation of Equilibrium

In Fig.1(a), a schematic diagram of a thin film with Ge deposition layers on a viscous layer and a substrate is presented. The coordinate system is also given. The bending elastic energy per unit width of a thin film, which is modeled as a plate bending into a cylindrical surface[23], is given as follows:

$$U = \int_0^L \frac{1}{2} E^* I \left(\frac{\mathrm{d}^2 w}{\mathrm{d}x^2} \right)^2 \mathrm{d}x \tag{1}$$

where L is the thin film length, E^* the effective Young's modulus defined as $E^* = E/(1-\nu^2)$[16,18,19]. E, ν are the Young's modulus and the Poisson's ratio of the thin film, respectively. I is the area moment of inertia per unit width defined as $I = h^3/12$, and h is the film thickness. w is the film deflection.

Figure 1(b) illustrates the stress and moment exerted by the Ge deposition layers/dots on the film. Inside the thin film, the load per unit width P is assumed to have the following distribution

$$P(w,x) = P_1(w,x) + P_2 + \sum_{k=1}^{Q} S_k J_k(x) \tag{2}$$

$P_1(w,x)$ is the constraint load, which is unknown yet and we will talk about it later in details. P_2 is the load per unit width due to the constant residual stress inside the film. Q is the number of the deposition layers/dots. S_k is the load per unit width induced by the lattice mismatch of Ge and Si at the bimaterial interface. Here S_k is assumed to be uniformly distributed along the Si/Ge interface and function $J_k(x)$ has the following definition

$$J_k(x) = \begin{cases} x_k^e - x_k^s = d_k & (x_k^s) \\ x - x_k^s & (x_k^s \le x \le x_k^e) \\ 0 & (x < x_k^s) \end{cases} \tag{3}$$

x_k^s, x_k^e are the starting and ending coordinates of the kth deposition layer. d_k is the length of the kth deposition layer and $d_k = x_k^e - x_k^s$. $P > 0$ is tensile and $P < 0$ is compressive. The external work W_1 due to P is as follows

$$W_1 = -\int_0^L \frac{P}{2} \left(\frac{\mathrm{d}w}{\mathrm{d}x} \right)^2 \mathrm{d}x \tag{4}$$

The uniformly distributed bending moment m_k due to S_k is defined as[24]

$$m_k = \frac{S_k h}{2} \tag{5}$$

The external work W_2 due to this bending moment is[24]

$$W_2 = \int_0^L \sum_{k=1}^{Q} m_k \phi_k(x) \frac{\mathrm{d}^2 w}{\mathrm{d}x^2} \mathrm{d}x \tag{6}$$

$\phi_k(x)$ is the function defined as

$$\phi_k(x) = H(x - x_k^s) - H(x - x_k^e) \tag{7}$$

in which H is the Heaviside function defined as

$$H(x - x_o) = \begin{cases} 1 & (x > x_o) \\ 0 & (x \le x_o) \end{cases} \tag{8}$$

where x_o is a constant. The purpose of introducing the Heaviside function is to define the action domain of the deposition layer, which is similar to the case of using the Heaviside function to differentiate the cracked and uncracked area in Ref.[25]. The above modeling of the effect of the interfacial stress is from the third model presented in Ref.[24], which in essence is a local stressor model[11,26].

The external work of W_3 due to the pressure exerted by the viscous layer of q is as follows:

$$W_3 = \int_0^L \int_0^w q \, \mathrm{d}w \mathrm{d}x \tag{9}$$

By applying the principle of virtual work (PVW), i.e., $\delta(U - W) = 0 \quad (W = W_1 + W_2 + W_3)$, the equation of equilibrium is derived as the following:

$$E^* I \frac{\mathrm{d}^4 w}{\mathrm{d}x^4} - \left(P \frac{\mathrm{d}^2 w}{\mathrm{d}x^2} + \frac{\mathrm{d}P}{\mathrm{d}x} \frac{\mathrm{d}w}{\mathrm{d}x} \right) - \sum_{k=1}^{Q} m_k \frac{\mathrm{d}^2 \phi_k}{\mathrm{d}x^2} = q \tag{10}$$

The definition of ϕ_k is shown in Eq.(7) and $\dfrac{\mathrm{d}^2 \phi_k}{\mathrm{d}x^2} = \dfrac{\mathrm{d}\delta(x - x_k^s)}{\mathrm{d}x} - \dfrac{\mathrm{d}\delta(x - x_k^e)}{\mathrm{d}x}$. Here $\delta(x - x_o)$ is the Dirac delta function. For the detailed derivation of q from the lubrication theory and the Stokes flow, the reader is referred to the papers of Huang and Suo[18,19]. Here we define q has such a form as $q = -\kappa w$ which is the Winkler elastic foundation model for a viscous layer. κ is the modulus of the elastic foundation and is assumed constant here. In conjunction with Eqs.(23) and (27) in Ref.[18], it is not difficult to find out that $\kappa = \sigma_o h k_w^2 + \dfrac{E k_w^4 h^3}{12(1 - \nu^2)}$ (σ_o is a compressive axial stress and k_w is the wave number of the buckled film) for a viscous layer modeled by the lubrication theory. Similarly, in conjunction with Eqs.(19) and (23) in Ref.[19], $\kappa = \dfrac{E h k_w^2}{12(1 - \nu^2)} [12(1+\nu)\varepsilon_o + (k_w h)^2]$ (ε_o is a compressive axial strain) for a viscous layer modeled as the Stokes flow. Because $\sigma_o = E\varepsilon_o(1 - \nu)$[18], the elastic foundation moduli of a viscous layer modeled by the lubrication theory and the Stokes flow are the same. However, the flows of the above two models are different and therefore their temporal evolutions are different in a non-equilibrium study[18,19]. It is also noticed that once we set the bending moment $m_k = 0$, Eq.(10) recovers the governing equation of the buckling analysis presented by Huang and Suo [18,19]. It is this bending moment m_k which makes the film deflect no matter what the axial load P is. So far, we still can not solve Eq.(10) because of the unknown feature of the constraint force $P_1(P)$.

The question now is how to solve P_1. When a plate bends into a cylindrical surface and its edges are free of constraints, there is a (compressive) displacement of $\displaystyle\int_0^L \frac{1}{2} \left(\frac{\mathrm{d}w}{\mathrm{d}x} \right)^2 \mathrm{d}x$ due to the plate deflection. The displacement due to the axial load P is $\displaystyle\int_0^L \frac{P}{E^* h} \mathrm{d}x$. The following equation states the constraint of immovable edges[23]

$$\int_0^L \frac{P}{E^* h} \mathrm{d}x = \int_0^L \frac{1}{2} \left(\frac{\mathrm{d}w}{\mathrm{d}x} \right)^2 \mathrm{d}x \tag{11}$$

P_1 can thus be solved by this constraint equation once w is known. In computation, we first guess a P_1 value in Eq.(10), solve w and substitute it into Eq.(11) to solve P_1, and then substitute this newly solved P_1 back into Eq.(10) again. The above procedure is repeated until both P_1 and w are converged. Here it is also worth pointing out that the above modeling is for a small deflection analysis and the nonlinear influence of membrane stretching[27] is not considered. For a free-standing structure the nonlinear membrane stretching will stiffen the structure[27]. For the film/viscous layer/substrate system studied here, besides the stiffening effect, the membrane stretching will have significant impact on the constraint force especially when the local bending is severe.

2.2. Nondimensionalization and Numerical Solution

In order to nondimensionalize Eqs.(10) and (11), the following dimensionless numbers are introduced[28]

$$\xi = \frac{x}{L}, \quad W = \frac{w}{L}, \quad \xi_k^s = \frac{x_k^s}{L}, \quad \xi_k^e = \frac{x_k^e}{L}, \quad D_k = \frac{d_k}{L} \tag{12}$$

And for simplicity reasons, we let $S_k = S$ and $D_k = D$ $(k = 1, 2, ..., Q)$. Equation (10) is now nondimensionalized as the following

$$W'''' - \left[\alpha_1 + \alpha_2 + \alpha_3 \sum_{k=1}^{Q} J_k(\xi) \right] W'' + \alpha_3 \sum_{k=1}^{Q} \phi_k(\xi) W' - \frac{\alpha_3}{2} \sum_{k=1}^{Q} \phi_k''(\xi) = \alpha_4 W \tag{13}$$

Now Eq.(11) becomes as follows after some simple manipulations

$$\alpha_1 = 6\int_0^1 W'^2 \mathrm{d}\xi - \alpha_2 - \alpha_3 \sum_{k=1}^{Q}\left[D(1-\xi_k^e) + \frac{D^2}{2}\right] \tag{14}$$

Here $()' = \mathrm{d}/\mathrm{d}\xi$. α_i ($i = 1$ to 4) is defined as follows:

$$\alpha_1 = \frac{P_1 L^2}{E^* I}, \quad \alpha_2 = \frac{P_2 L^2}{E^* I}, \quad \alpha_3 = \frac{SL^3}{E^* I}, \quad \alpha_4 = \frac{\kappa L^4}{E^* I} \tag{15}$$

To solve Eq.(13), we assume that W has the sine series expansion for a hinged-hinged film bending into a cylindrical surface[29]

$$W = \sum_{j=1}^{M} a_j \sin(j\pi\xi) \tag{16}$$

M is the mode number. a_j is the modal amplitude to be determined. This sine series expansion of W also implicitly indicates that the thin film is not delaminated at the edges because $\sin(j\pi\xi) = 0$ at $\xi = 0$ and 1. It is worth pointing out that during the derivation of governing Eq.(13), we implicitly assume that $\mathrm{d}P_1/\mathrm{d}x = 0$ (or $\mathrm{d}P_1/\mathrm{d}\xi = 0$), which means the constraint axial load P_1 is distributed uniformly through the whole film domain. In reality P_1 should vary at different ξ. However, it will be extremely difficult, if not impossible, to find a function of P_1 varying with ξ. The integral constraint equation of (11) is just an overall constraint condition of requiring the whole thin film to generate a matching constraint force to comply with the compatibility condition. It is a convenient way of assuming P_1 is a constant for each deflection configuration of w.

We now substitute W of Eq.(16) into Eq.(13), multiply it by $\sin(j\pi\xi)$ and integrate it from 0 to 1. Equation (13) becomes as the following:

$$\boldsymbol{C}\boldsymbol{A} = \boldsymbol{V} \tag{17}$$

$\boldsymbol{C}$ is the matrix with its element defined as

$$\begin{aligned} C_{ij} = \int_0^1 \sin(i\pi\xi)\Bigg\{ & \sin''''(j\pi\xi) - \left[\alpha_1 + \alpha_2 + \alpha_3 \sum_{k=1}^{Q} J_k(\xi)\right]\sin''(j\pi\xi) \\ & + \alpha_3 \sum_{k=1}^{Q} \phi_k(\xi)\sin'(j\pi\xi) - \alpha_4 \sin(j\pi\xi)\Bigg\}\mathrm{d}\xi \quad (i,j = 1,2\cdots,M) \end{aligned} \tag{18}$$

$\boldsymbol{A}$ and $\boldsymbol{V}$ are vectors defined as $\boldsymbol{A}^{\mathrm{T}} = \{a_1, a_2, a_3, \cdots, a_M\}$ and $\boldsymbol{V}^{\mathrm{T}} = \{V_1, V_2, V_3, \cdots, V_M\}$. V_i ($i = 1, 2, 3, ..., M$) has the following expression

$$\begin{aligned} V_i &= \int_0^1 \frac{\alpha_3 \sin(i\pi\xi)}{2} \sum_{k=1}^{Q} \phi_k''(\xi)\mathrm{d}\xi = \int_0^1 \frac{\alpha_3 \sin(i\pi\xi)}{2} \sum_{k=1}^{Q} [\delta'(\xi - \xi_k^s) - \delta'(\xi - \xi_k^e)]\mathrm{d}\xi \\ &= \frac{\alpha_3(i\pi)}{2} \sum_{k=1}^{Q} [\cos(i\pi\xi_k^s) - \cos(i\pi\xi_k^e)] \end{aligned} \tag{19}$$

In the above derivation, the following integral property of the Dirac delta function is used[30]

$$\int_0^1 f(x)\delta^{(n)}(x - x_o) = (-1)^{(n)} f^{(n)}(x_o) \qquad (0 \le x_o \le 1) \tag{20}$$

Here $\delta^{(n)}(x - x_o) = \mathrm{d}^n\delta(x - x_o)/\mathrm{d}x^n$ and $f^{(n)}(x_o) = \mathrm{d}^n f/\mathrm{d}x^n(x_o)$.

III. RESULTS AND DISCUSSIONS

In all the cases studied here, α_2 and α_3 are set as -1 and 10. α_3 is set to be positive, which physically means that the Ge deposition exerts tensile stress on the thin film[5]. The deposition dot length D is set as 0.01. Because α_1 is an unknown parameter, we first guess an α_1 value in Eq.(17) and solve α_1 via Eq.(14), and then substitute it into Eq.(17) again. The above procedure continues until both W and α_1 are converged. In Fig.2, 4 cases of thin film deflections with different deposition positions and numbers are presented. For each case, the deposition has the following distribution

$$\xi_k^s = \frac{1+4(k-1)}{2(2N-1)} - \frac{D}{2}, \quad \xi_k^e = \xi_k^s + D \qquad (k = 1, 2, \cdots, Q) \tag{21}$$

N is an integer. The whole purpose of designing such a deposition distribution is to let each deposition layer center located at the peaks of $\sin[(2N-1)\pi\xi]$. $\sin[(2N-1)\pi\xi]$ is the mode shape symmetric to $\xi = 1/2$. In Fig.2, N is taken as 2, 3, 4, 5 and the corresponding deposition layer number Q is $Q = N$. Clearly the local bending effects of $N = 2$ and $N = 4$ are much more severe than those of $N = 3$ and $N = 5$. That of $N = 4$ has more severe local bending than that of $N = 3$ indicates that when the number of deposition layers/dots is relatively small, increasing deposition density/number (at specific locations) may not reduce the local bending. The following fact may help to explain why $N = 2$ and $N = 4$ have larger local bending. For $N = 2$ and $N = 4$, $\xi = 1/2$ is the valley of their mode shapes of $\sin[(2N-1)\pi\xi]$ and there is no deposition layer/dot at $\xi = 1/2$. For $N = 3$ and $N = 5$, $\xi = 1/2$ is the peak of their mode shapes of $\sin[(2N-1)\pi\xi]$ and there is a deposition layer/dot at $\xi = 1/2$. $N = 5$ shows an overall extended bending. It is also noticed that because of the localization effects of the stress and moment exerted by the deposition dots, a large mode number of M is needed to approximate the deflection shape for the computation convergence.

In Fig.3, the influence of the deposition layer/dot position is studied. The number of deposition layer Q is fixed as 2 and the thin film deflection evolution as a function of the positions of the two deposition layers are presented. We first define that the deposition has the following distribution

$$\xi_k^s = \frac{1+4(k-1)}{2(2N-1)} + \psi_k \varepsilon_{\text{shift}} - \frac{D}{2}, \quad \xi_k^e = \xi_k^s + D \qquad (k = 1, 2) \tag{22}$$

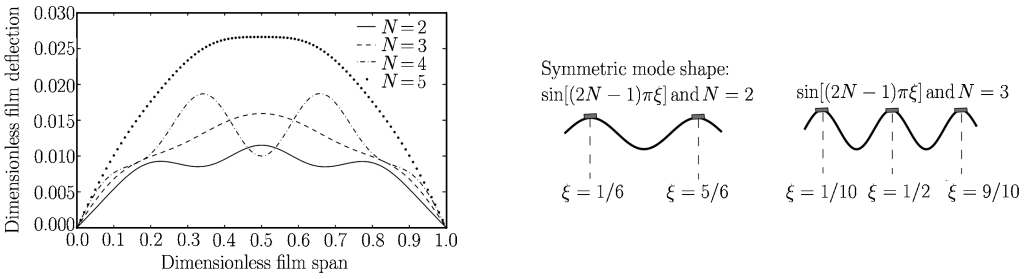

Fig. 2. The evolution of thin film deflection as the Ge deposition layer number Q increases. The Ge deposition layer centers are located at the peaks of symmetric mode shape of $\sin[(2N-1)\pi\xi]$ and $N = 2$, 3, 4, 5, respectively.

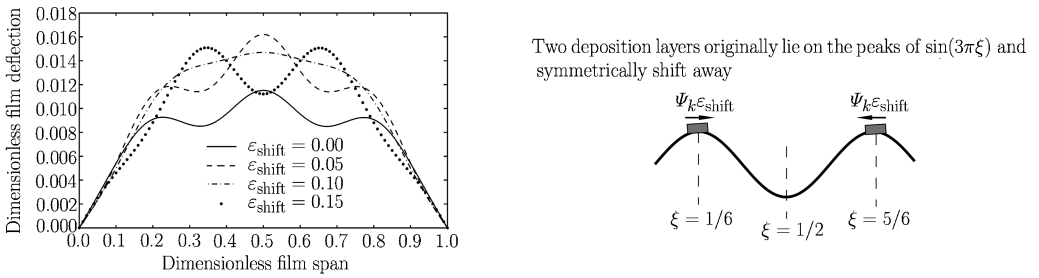

Fig. 3. The evolution of thin film deflection as the two Ge deposition layers symmetrically shift away from the two peaks of the mode shape of $\sin(3\pi\xi)$, which are located at $\xi = 1/6$ and $\xi = 5/6$, respectively.

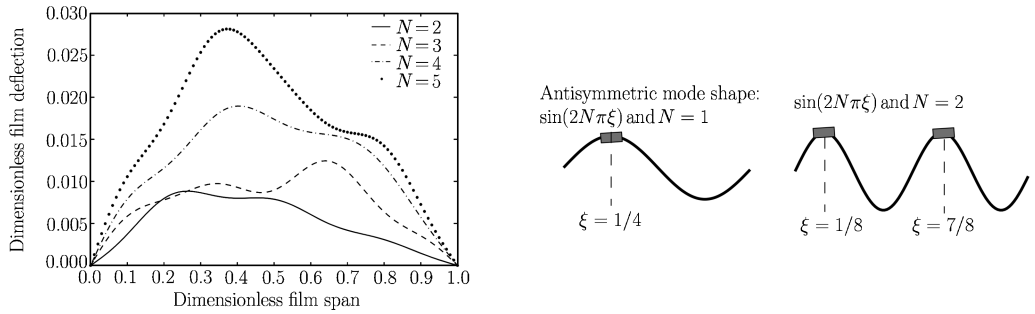

Fig. 4. The evolution of thin film deflection as the Ge deposition number Q increases. The Ge deposition layer centers are located at the peaks of an anti-symmetric mode shape of $\sin(2N\pi\xi)$ and $N = 1$, 2, 3, 4, respectively.

N and Q are fixed as 2. ψ_k is the function defined as follows:

$$\psi_k = \begin{cases} 1, & \xi_k^s + D/2 < 0.5 \\ 0, & \xi_k^s + D/2 = 0.5 \\ -1, & \xi_k^s + D/2 > 0.5 \end{cases} \tag{23}$$

The purpose of defining function ψ_k is to let the two deposition positions shift symmetrically towards $\xi = 1/2$. Physically, $\varepsilon_{\text{shift}}$ is thus the shift displacement of the deposition layer(s) away from the film center. At the beginning, the two depositions are located at the two peaks of $\sin(3\pi\xi)$ at $\xi = 1/6$ and $\xi = 5/6$, which is the $\varepsilon_{\text{shift}} = 0$ case. In Fig.3, $\varepsilon_{\text{shift}}$ is taken as 0, 0.05, 0.1 and 0.15. Figure 3 shows that such a deposition shift does not necessarily reduce the local bending, either.

Figures 2 and 3 deal with the symmetric case. Now let us look at the local bending effect of the depositions on the peaks of an anti-symmetric mode shape. In Fig.4 the deposition has the following distribution

$$\xi_k^s = \frac{1 + 4(k-1)}{4N} + \psi_k \varepsilon_{\text{shift}} - \frac{D}{2}, \quad \xi_k^e = \xi_k^s + D \qquad (k = 1, 2, \cdots, Q) \tag{24}$$

Such a distribution is designed to let the deposition layer/dot center at the peaks of the anti-symmetric mode shape of $\sin(2N\pi\xi)$. N is set as 1, 2, 3 and 4 and accordingly $Q = N$. All the cases in Fig.4 show asymmetric deflections. The reason is simple. For example, as $N = 1$, there is only one peak at $\xi = 1/4$ and one valley at $\xi = 3/4$ for the mode shape of $\sin(2\pi\xi)$. So such deposition breaks the anti-symmetry of $\sin(2\pi\xi)$ and makes the deflection asymmetric. There is some trend that the local bending effect is weakened as the deposition number $Q\,(Q = N)$ increases.

Figures 2, 3 and 4 all set the deposition layers at or around the peaks of a sinusoid. Now we study more general cases that the deposition layers are set at or around both the peaks and valleys of a sinusoid. In Fig.5 the deposition layers/dots center at both the peaks and valleys of the symmetric mode shape of $\sin[(2N-1)\pi\xi]$. N is set as 2, 3, 4 and 5. The corresponding deposition number $Q = 2N - 1$ because there are totally $2N-1$ peaks and valleys for $\sin[(2N-1)\pi\xi]$. Clearly as the deposition density/number

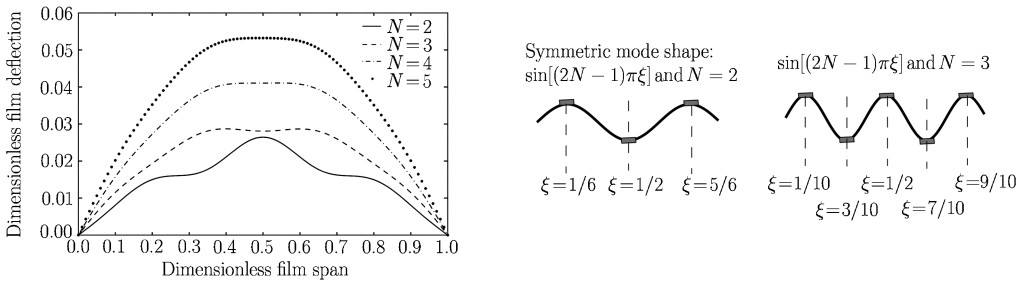

Fig. 5. The evolution of thin film deflection as the Ge deposition number Q increases. The Ge deposition layer centers are located at the both peaks and valleys of symmetric mode shape of $\sin[(2N-1)\pi\xi]$ ($N = 2$, 3, 4, 5).

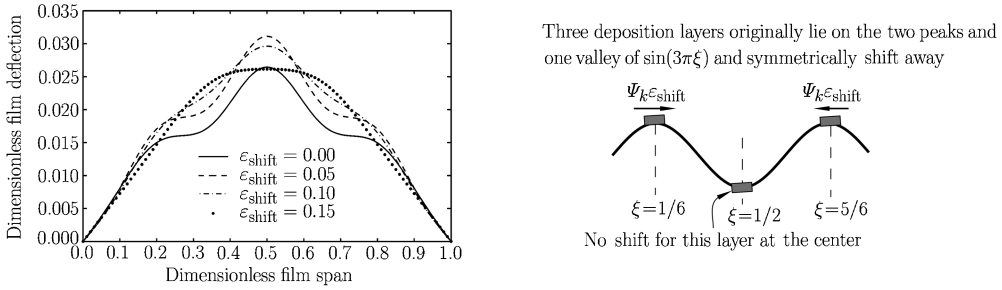

Fig. 6. The evolution of thin film deflection as three Ge deposition layers symmetrically shift away from the two peaks and one valleys of the mode shape of $\sin(3\pi\xi)$.

increases, the local bending of the thin film is steadily reduced and the thin film deflection evolves to overall extended bending shapes, which agrees with the experimental report by Liu et al.[11].

In Fig.6, we study the thin film deflection evolution when the deposition number Q is fixed as 3 and deposition positions gradually shift towards the center. The deposition position has the following distribution

$$\xi_k^s = \frac{1+2(k-1)}{2(2N-1)} + \psi_k\varepsilon_{\text{shift}} - \frac{D}{2}, \quad \xi_k^e = \xi_k^s + D \qquad (k = 1, 3) \tag{25}$$

At the beginning, the depositions locate at the peaks and valley of $\sin(3\pi\xi)$ at $\xi = 1/6$ (peak), $\xi = 1/2$ (valley) and $\xi = 5/6$ (peak). $\varepsilon_{\text{shift}}$ is taken as 0, 0.05, 0.1 and 0.15. For these cases, the local bending effect is also steadily reduced as the depositions shift towards the center.

IV. CONCLUDING REMARKS

The influences of different deposition densities/numbers and positions on the local bending of the thin film are studied. We show that for the case the depositions located only at the symmetric peaks, the density increase or position shift does not necessarily reduce the local bending effect. Depositions on the peaks of symmetric and anti-symmetric mode shapes induce quite different deflections. When the deposition layers/dots center at or around both the peaks and valleys of a mode shape, the density increase or deposition position shifting away from the peaks and valleys steadily reduces the local bending effect, and the film evolves to an overall extended bending shape.

Liu et al.[11] reported that the Ge deposition shape (thickness) also affects the local bending. In this paper, the deposition contribution to the thin film bending stiffness is not considered and the stress induced at the Ge/Si bimaterial interface is assumed uniform. During Stranski-Krastanow (SK) or Volmer-Weber (VW) growth, islands (dots) formation tends to relax elastic strain and the resulting strain/stress fields are highly non-uniform[31]. Although our equation of equilibrium is derived by assuming that the interfacial stress is uniformly distributed, the model itself is capable of describing the non-uniformly distributed stress scenario.

References

[1] Medeiros-Ribeiro,G., Braykovsky,A.M., Kamins,T.I., Ohlberg,D.A.A. and Williams,R.S., Shape transition of Ge nanocrystals on Si(001): from pyramids to domes. *Science,* 1998, 279: 353-355.

[2] Floro,J.A., Chason,E., Sinclair,M.B., Freund,L.B. and Lucadamo,G.A., Dynamic self-organization of strained islands during SiGe epitaxial growth. *Applied Physics Letters*, 1998, 73(7): 951-953.

[3] Ross,F.M., Tersoff,J. and Tromp,R.M., Coarsening of self-assembled Ge quantum dots on Si(100). *Physical Review Letters*, 1998, 80(5): 984-987.

[4] Floro,J.A., Chason,E., Freund,L.B., Twesten,R.D., Hwang,R.Q. and Lucadamo,G.A., Evolution of coherent islands in Si1-xGex/Si(001). *Physical Review B*, 1999, 59: 1990-1998.

[5] Kim,H.J. and Xie,Y.H., Influence of the wetting-layer growth kinetics on the size and shape of Ge self-assembled quantum dots on Si(001). *Applied Physics Letters*, 2001, 79(2): 263-265.

[6] Jin,G., Liu,J.L. and Wang,K.L., Temperature effect on the formation of uniform self-assembled Ge dots. *Applied Physics Letters*, 2003, 83(14): 2847-2849.

[7] Lo,Y.H., New approach to grow pseudomorphic structure over the critical thickness. *Applied Physics Letters,* 1991, 59(18): 2311-2313.

[8] Yin,H., Huang,R., Hobart,K.D., Suo,Z., Kuan,T.S., Inoki,C.K., Shieh,S.R., Duffy,T.S., Kub,F.J. and Sturm,J.C., Strain relaxation of SiGe islands on compliant oxide. *Applied Physics Letters*, 2002, 91(12): 9716-9722.
[9] Barvosa-Carter,W. and Aziz,M.J., Kinetically driven instability in stressed solids. *Physical Review Letters,* 1998, 81(7): 1445-1448.
[10] Gerling,M., Gustafsson,A., Rich,D.H., Ritter,D. and Gershoni,D., Roughening transition and solid-state diffusion in short-period InP/In0.53Ga0.47 as superlattice. *Applied Physics Letters*, 2001, 78(10): 1370-1372.
[11] Liu,F., Rugheimer,P., Mateeva,E., Savage,D.E. and Lagally,M.G., Response of a strained semiconductor structure. *Nature*, 2002, 416: 498.
[12] Asaro,R.J. and Tiller,W.T., Interface morphology development during stress corrosion cracking — Part I. via surface diffusion. *Metallurgical and Materials Transactions B,* 1972, 3(7): 1789-1796.
[13] Srolovitz,D.J., On the stability of surfaces of stressed solids. *Acta Metallurgica*, 1989, 37(2): 621-625.
[14] Liau,Z.L., Strained interface of lattice-mismatched wafer fusion. *Physical Review B*, 1997, 55(19): 12899-12901.
[15] Zhang,Y., Analysis of dislocation-induced strain field in an idealized wafer-bonded microstructure. *Journal of Physics D: Applied Physics,* 2007, 40: 1118-1127.
[16] Sridhar,N., Srolovitz,D.J. and Suo,Z., Kinetics of buckling of a compressed film on a viscous substrate. *Applied Physics Letters,* 2001, 78(17): 2482-2484.
[17] Yang,W.H. and Srolovitz,D.J., Cracklike surface instabilities in stressed solids. *Physical Review Letters,* 1993, 71(10): 1593-1596.
[18] Huang,R. and Suo,Z., Wrinkling of a compressed elastic film on a viscous layer. *Journal of Applied Physics,* 2002, 91(3): 1135-1142.
[19] Huang,R. and Suo,Z., Instability of a compressed elastic film on a viscous layer. *International Journal of Solids and Structures*, 2002, 39: 1791-1802.
[20] Huck,W.T.S., Bowden,N., Onck,P., Pardoen,T., Hutchinson,J.W. and Whitesides,G.M., Ordering of spontaneously formed buckles on planar surfaces. *Langmuir*, 2000, 16(7): 3497-3501.
[21] Bowden,N., Brittain,S., Evans,A.G., Hutchinson,J.W. and Whitesides,G.M., Spontaneous formation of ordered structures in thin films of metals supported on an elastomeric polymer. *Nature*, 1998, 393: 146-149.
[22] Zhang,Y. and Zhao,Y., Applicability range of Stoney's formula and modified formulas for a film/substrate bilayer. *Journal of Applied Physics*, 2006, 99: 053513.
[23] Timoshenko,S. and Woinosky-Krieger,S., Theory of Plates and Shells, 2nd edn. New York: McGraw-Hill Book Company, 1959.
[24] Zhang,Y. and Zhao,Y., Modelling analysis of surface stress on a rectangular cantilever beam. *Journal of Physics D: Applied Physics*, 2004, 37: 2140-2145.
[25] Zhang,Y. and Murphy,K., Crack propagation in structures subjected to periodic excitation. *Acta Mechanica Solida Sinica*, 2007, 20(3): 236-246.
[26] Evans,D.R. and Craig,V.S.J., The origin of surface stress induced by adsorption of iodine on gold. *Journal of Physical Chemistry B*, 2006, 110: 19507-19514.
[27] ZhangY. and Zhao,Y., An effective method of determining the residual stress gradients. *Microsystem Technologies,* 2004, 12: 357-364.
[28] Zhang,Y. and Zhao,Y., Static study of cantilever beam stiction under electrostatic force influence. *Acta Mechanica Solida Sinica,* 2004, 17(2): 104-111.
[29] Timoshenko,S., Theory of Elastic Stability, 1st edn. Engineering Societies Monographs, 1936.
[30] Colwell,D.J.and Gillett,J.R., A property of the Dirac delta function. *International Journal of Mathematical Education in Science and Technology*, 1986, 18: 637-638.
[31] Johnson,H.T. and Freund,L.B., Mechanics of coherent and dislocated island morphologies in strained epitaxial material system. *Journal of Applied Physics*, 1997, 81(9): 6081-6090.